AURORA AND AURORAL PARTICLES

Kazuo MAKITA

Takushoku University, 4–14, Kohinata 3-chome, Bunkyo-ku, Tokyo 112

Abstract: Electron precipitation observed by DMSP is categorized into five fundamental types in relation to its possible sources as follows:

(1) Plasma sheet electrons related to discrete auroras and transpolar θ auroras: The energy spectra of this precipitation show a clear peak electron number flux at some energy between 1 to 10 keV.

(2) Plasma sheet electrons related to diffuse auroras: The characteristics of energy spectra of this kind of precipitation have no clear peak number flux in the energy range from 50 eV to 20 keV but have high energy tail.

(3) Magnetospheric boundary layer electron related to sun-aligned arcs and/or faint arcs: The energy spectra have a clear peak in the electron number flux at about a few hundred eV.

(4) Polar cusp electrons related to dayside soft precipitation: The cusp precipitation is characterized by a large electron number flux and is low energy (less that 100 eV).

(5) Magnetospheric tail lobe electron related to polar rain: The spectra of these electrons are identical in shape with cusp electron but are generally lower in intensity by about 1–2 orders of magnitude.

The spatial distribution of these electron precipitation regions depends on the magnitude of geomagnetic activity and on the IMF polarity, and gives us important information about the solar wind–magnetosphere interaction.

1. Introduction

Recent satellite observations have provided us with much data for a more accurate understanding of magnetospheric structure and auroral phenomena. Multiple spacecraft equipped with particle detectors, launched during the International Magnetospheric Study (IMS) period, gave us valuable information about particle precipitation pattern. BURKE (1982) reviewed the recent observations of particle precipitation and REIFF (1983) summarized the auroral morphology and precipitating particle patterns determined during the IMS period.

Various kinds of particle precipitation observed at low altitude are reported by many researchers: These include discrete and diffuse auroras (LUI *et al.*, 1977), θ auroras (FRANK *et al.*, 1982), sun-aligned arcs (LASSEN and DANIELSEN, 1978), soft and hard precipitation (SHARP and JOHNSON, 1968), cusp precipitation (FRANK, 1971), polar rain, polar showers, and polar squalls (WINNINGHAM and HEIKKILA, 1974). For example, WINNINGHAM and HEIKKILA (1974) showed that there are three different kinds of electron precipitation over the polar cap; they are polar rain, polar shower and polar squall. LASSEN and DANIELSEN (1978) observed the sun-aligned arcs at extremely high latitude and FRANK *et al.* (1982) also reported the transpolar θ auroras

over the polar cap. However, the correspondence between precipitation in the polar cap and the polar cap auroras is not yet known.

On the basis of electron data obtained by DMSP satellites, we examine various kinds of electron precipitation observed over the polar region and categorize them into five types by source.

The orbits of the DMSP F2 and F3 satellites were in the dawn-dusk meridian and that of the F4 satellite was in the noon-midnight meridian. These satellites were almost sun-synchronous with an altitude of 840 km and a period of 101.5 min for the time period examined here. The low-energy electron detector had a field of view of $10^\circ \times 15^\circ$ pointing toward the local geocentric zenith. It measured the precipitation of low-energy electrons between 50 eV and 20 keV in 16 energy channels by using two analyzers (HARDY *et al.*, 1979).

2. Auroral Electron Precipitation in the Dawn and the Dusk Sectors

In this chapter, we show typical examples of electron precipitation in the dawn and the dusk sectors during quiet and disturbed magnetic conditions.

2.1. Electron precipitation along the dawn-dusk meridian during a quiet period

An auroral image and electron precipitation observed by DMSP-F2 satellite during a quiet period are shown in Fig. 1. In this period the average hourly value of *AE* was smaller than 50 nT. The satellite traveled from the dusk ($\sim$19 MLT) to the dawn sector ($\sim$08 MLT) over the southern hemisphere in this period. The top panel shows electron precipitation data. From top to bottom the three plots are electron number flux, energy flux and average energy. The characteristics of the electron precipitation show that there are two different kinds of precipitation. One is that with a high average energy, in the region located at the equatorward side of the auroral oval (from 69° to 79° on the dusk side and from 68° to 77° on the dawn side), and the other is characterized by a low average energy located ($10^{-1} \sim 1$ keV) at the poleward side of auroral oval (from 79° to 84° in the dusk side and from 77° to 84° in the dawn side). The poleward boundary of the lower energy electron precipitation is generally located at a very high latitude near 84° during quiet times as shown in this figure.

The bottom panel shows the auroral image from this period. The dark region corresponds to the auroral luminous region. Comparing the precipitation with the auroral image, it is shown that the higher energy electron precipitation in the dusk sector corresponds to the bright discrete and diffuse aurora and the lower energy electron precipitation corresponds to a faint discrete aurora. This tendency is more clearly seen in the dawn sector; where, the higher energy electron precipitation corresponds to a diffuse aurora and the lower energy electron precipitation corresponds to the faint discrete aurora.

In order to clarify the characteristics of electron precipitation, the electron differential energy spectra are shown in Fig. 2. The energy spectra of electrons corresponding to the two regions in both the dawn and the dusk sectors are shown in this figure. It shows that the differential energy spectra corresponding to the faint

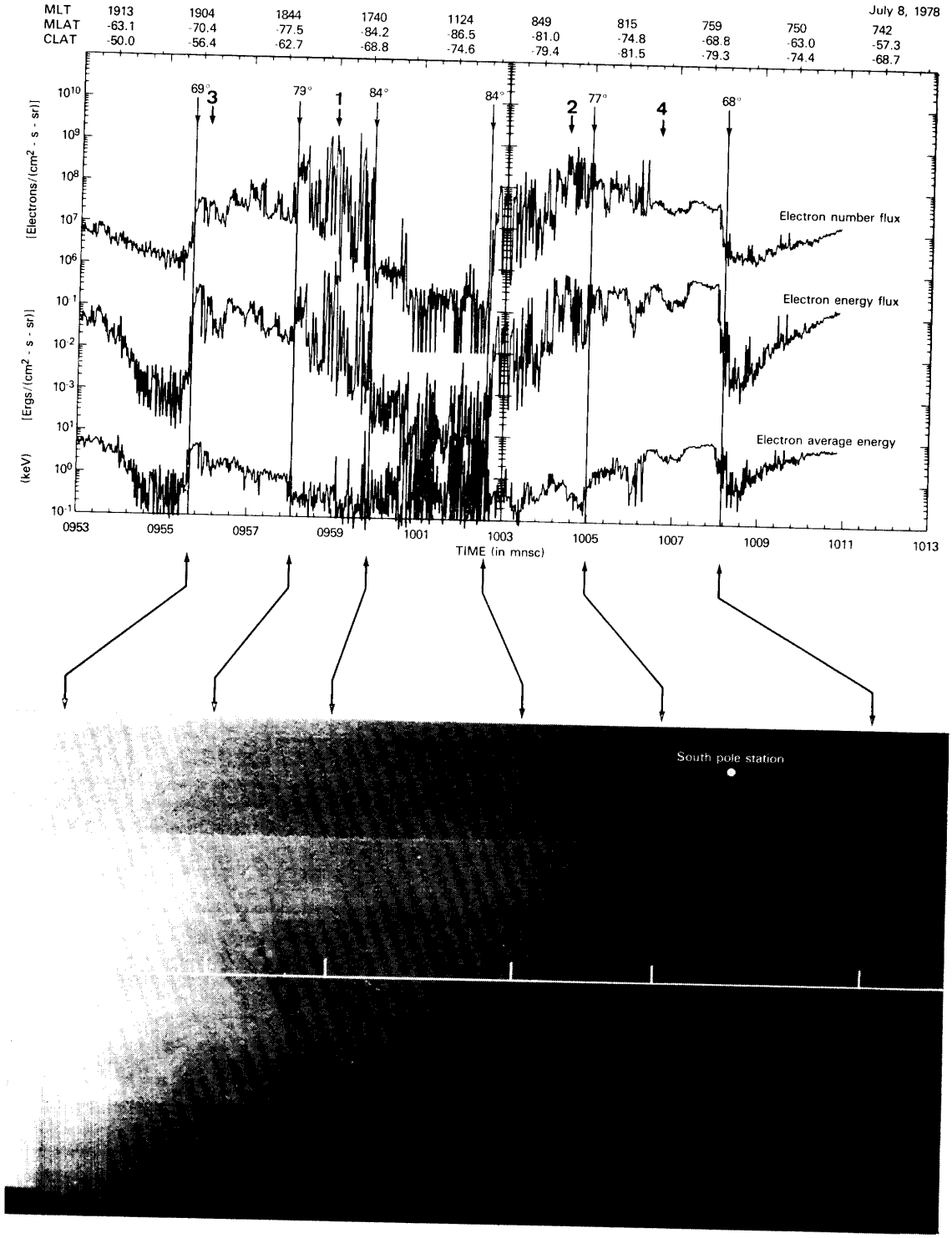

Fig. 1. Electron precipitation observed by the DMSP-F2 satellite and the simultaneous auroral photograph taken by the same satellite during a quiet period. The top panel shows the electron number flux, energy flux and average energy. The bottom panel shows the satellite imagery auroral photograph (in negative) with the white line depicting the satellite orbit where the auroral electron precipitations were measured. The electron differential spectra indicated by numbers 1–4 are shown in Fig. 2.

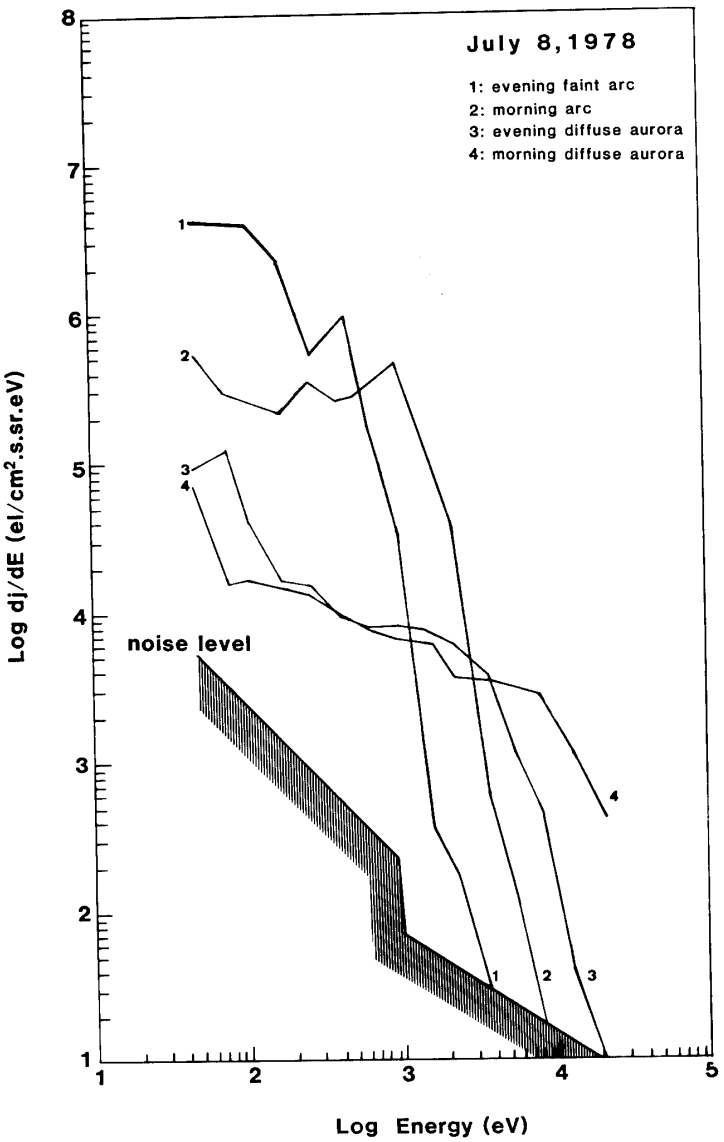

Fig. 2. Electron differential spectrum observed in the dawn and the dusk sectors during the quiet period. The discrete arc has a peak value at about 1 keV and the diffuse aurora spectrum has no clear peak flux value. The average electron energy of the discrete arc and the diffuse aurora in the morning sector is usually higher than that in the evening sector.

discrete auroral arc in both the dusk and the dawn sectors have peaks in the electron flux in the vicinity of 1 keV. The energy of the peak is a little lower than in the dusk sector and a little higher in the dawn sector.

On the other hand, it is evident that the differential energy spectra corresponding to the diffuse aurora in both the dawn and the dusk sectors have no clear peaks in the flux within the measured energy range, 50 eV to 20 keV. Note that the average energy of the electrons for both diffuse and discrete auroral regions is higher in the dawn sector than in the dusk sector during this quiet period.

2.2. Electron precipitation along the dawn-dusk meridian during a disturbed period

Electron precipitation and an auroral image obtained by DMSP-F2 satellite during a disturbed period are shown in Fig. 3. The hourly average value of *AE* was larger than 500 nT for the period of this time. The satellite traversed from the dusk to the dawn sector in the southern hemisphere. The top panel shows the distribution of electron precipitation. In this figure, it is evident that the enhanced electron precipitation regions are located at the lower latitude than during the quiet

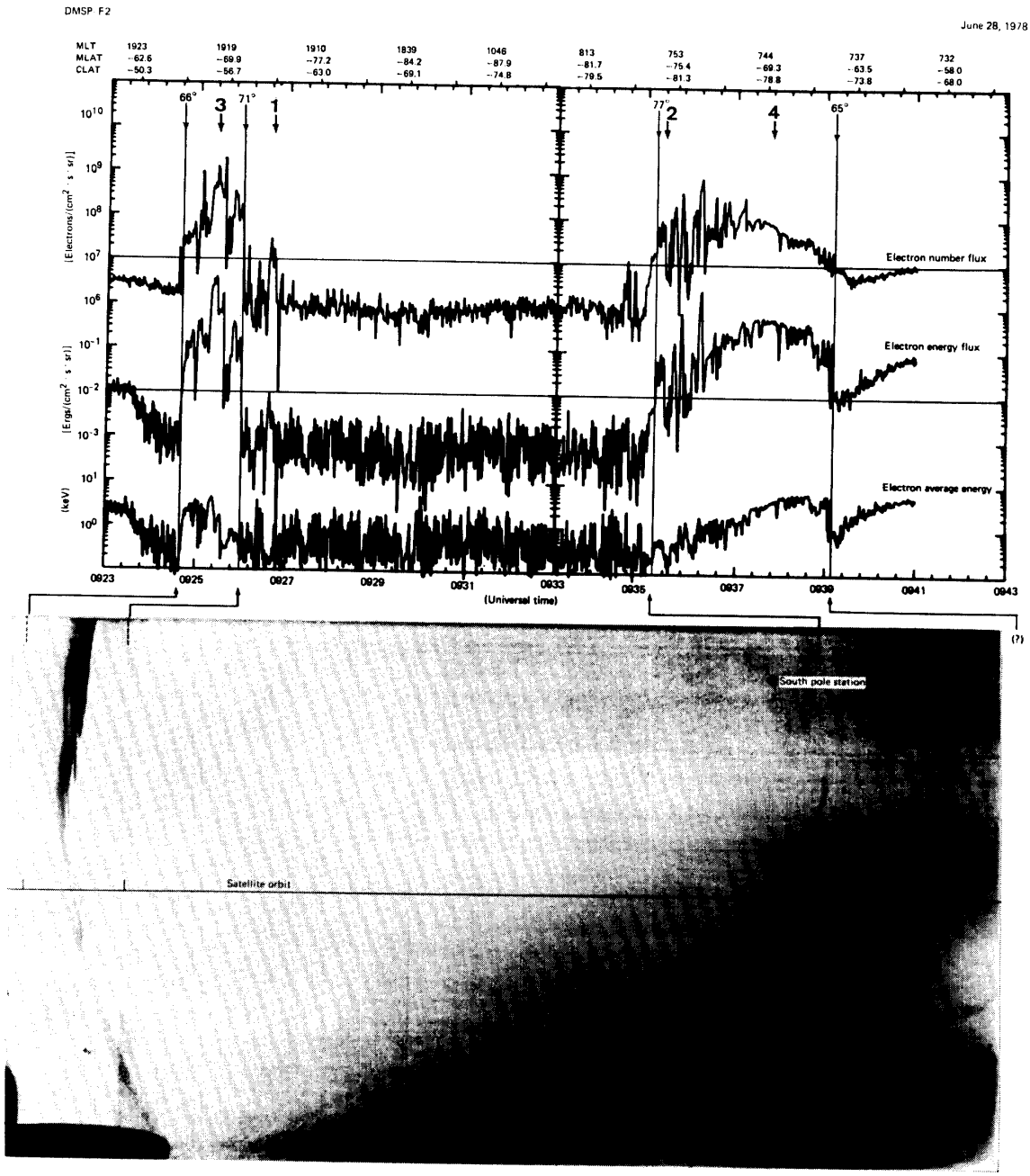

Fig. 3. Electron precipitation observed by the DMSP-F2 satellite and the simultaneous auroral photograph taken during a disturbed period. The format of this figure is the same as that of Fig. 1. The electron differential spectra indicated by numbers 1–4 are shown in Fig. 4.

period of Fig. 1. The hard electron precipitation regions extend from 66° to 71° and the soft electron precipitations cannot be recognized clearly in the dusk sector. In the dawn sector, the hard and the soft electron precipitation regions are seen from 65° to 74° and from 74° to 77°, respectively. It is noticed that electron precipitation with a low number flux (polar rain) can be seen at the higher latitude side of these electron precipitation regions. Generally, the polar rain region expands to the lower latitude area during disturbed periods (MAKITA *et al.*, 1983).

The bottom panel shows an auroral image obtained for the same time interval. This figure shows that the higher energy electron precipitate in a bright discrete auroral arc. The region, where the lower energy electrons precipitate, wide-spread during the quiet period, is not found in the dusk sector during this active period.

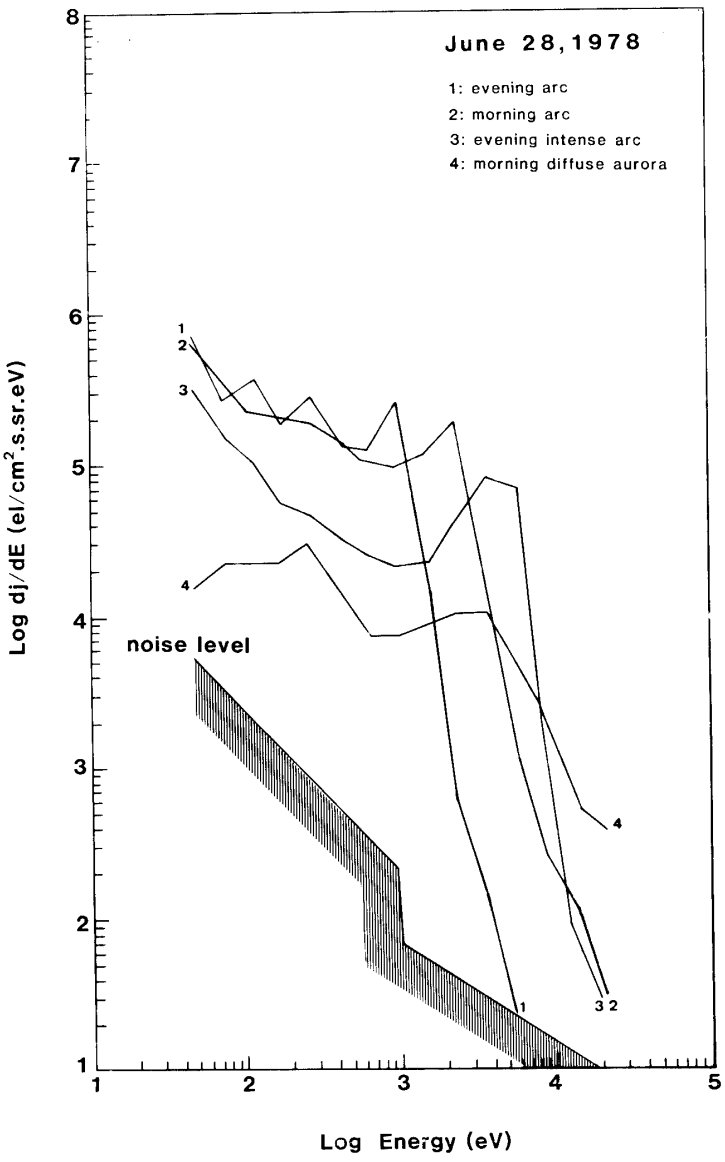

Fig. 4. Electron differential spectra observed in the dawn and the dusk sectors during the disturbed period. The discrete arc has a peak value at about a few keV and the auroral luminosity increases as the peak electron energy increases.

On the other hand, in the dawn sector, a discrete auroral arc is seen in the poleward side of the diffuse aurora. The characteristics of the auroral electron precipitation corresponding to these discrete and diffuse aurora are different. The precipitation above the discrete aurora consist of electrons with energies lower than a few keV and has a fluctuating spatial structure. The precipitation related to the diffuse aurora consists of electrons with energies of a few keV, a smooth, continuous spatial structure.

In order to clarify the characteristics of electron precipitation, several differential electron spectra are shown in Fig. 4. This figure shows that the energy of the peak flux appears to depend on the luminosity of discrete auroral arc. In the dusk sector, the differential energy spectrum of electrons observed above the faint discrete auroral arc has a peak at about 1 keV and the spectrum corresponding to the intense discrete arc has a peak at about 7 keV. The spectrum related to the discrete aurora in the dawn sector has a peak flux value at about 2 keV. This is consistent with the fact that the luminosity of the discrete aurora in the dawn sector appears to be between that of the intense and faint discrete auroras in the dusk sector. On the other hand, the precipitation related to the diffuse aurora has no clear peak flux value, extending up to 10 keV with a higher energy tail.

3. Electron Precipitation near the Dayside Sector

The electron precipitation near the dayside sector is characterized by high intensity electron fluxes with a low energy range ($<$300 eV). These particles are likely to come from the magnetosheath region and are precipitating directly to the cusp region (FRANK, 1971). We examine a typical example of cusp precipitation during a disturbed period.

Typical cusp precipitation in the dayside

Electron precipitation observed by DMSP-F4 satellite during a quiet period is shown in Fig. 5. The figure shows electron data obtained over the southern polar region during two orbits. The satellite traversed from the dayside to the nightside in these intervals. In the top panel, the enhanced electron precipitation region can be seen from 73° to 82° in the dayside and from 69° to 80° in the night side. The typical cusp precipitation is seen from 79° to 82° in the dayside region. The cusp precipitation is characterized by a high electron number flux ($10^9/cm^2 \cdot s \cdot sr$) and a low average energy ($<$300 eV). Although soft electron precipitation can be recognized in the nightside region from 75° to 80° in the top panel, the energy and flux characteristics of this electron precipitation are different from those in the cusp region. The electron number flux in the nightside region is lower and the average energy is higher compared to the dayside cusp precipitation. Similar characteristics of the precipitation can be seen in the bottom panel. Typical cusp precipitation is recognized from 78° to 84° in the dayside region in this panel. Low energy electron precipitation in the nightside sector, again shows a slightly higher average energy than that of the cusp precipitation.

Although the differences in the energy characteristics of cusp precipitation in the

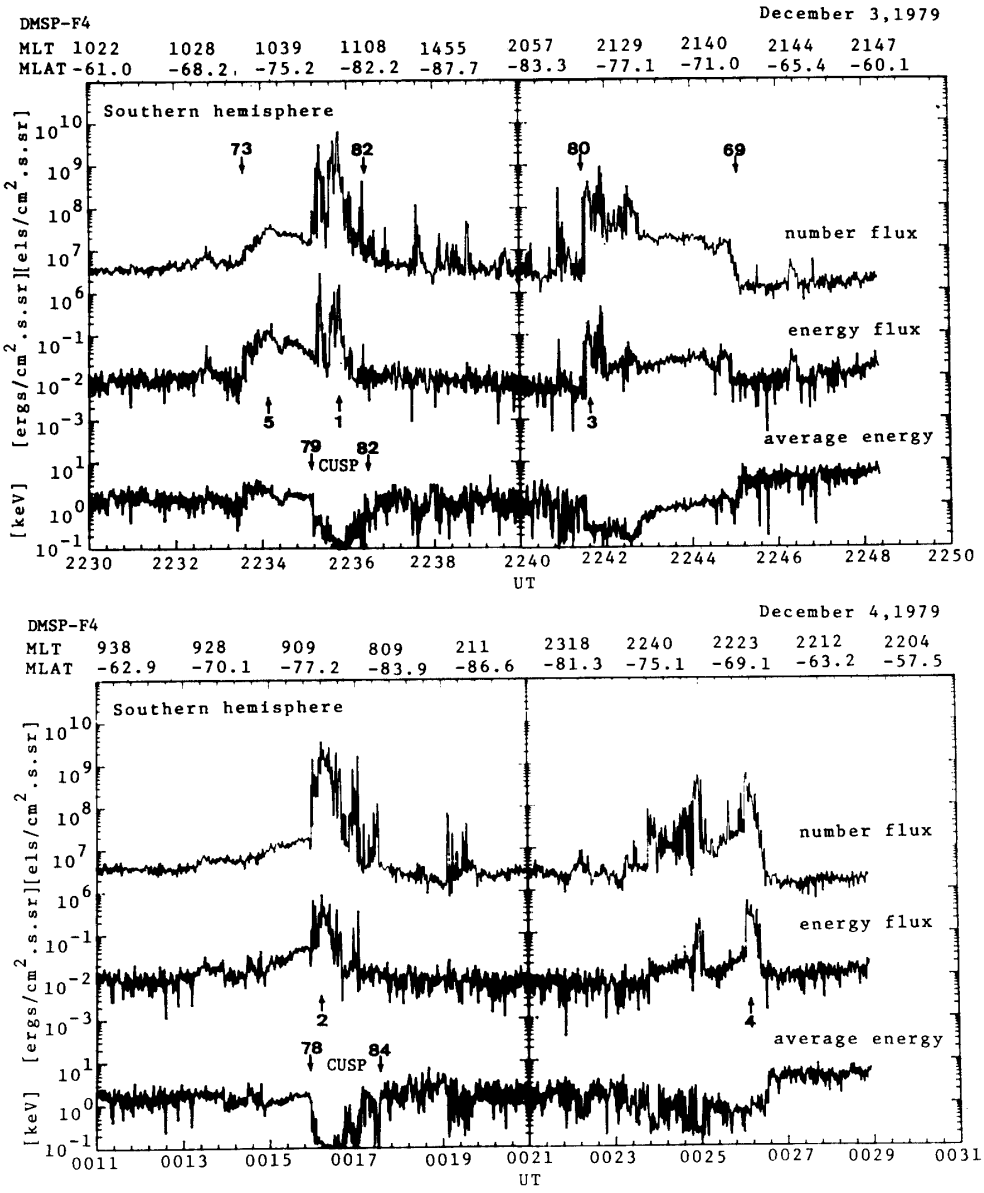

Fig. 5. The sequence electron precipitation data obtained by the DMSP-F4 satellite during 2230 to 2250 on December 3 and during 0011 to 0031 on December 4. Dayside cusp precipitation can be recognized from 79°–82° in the top panel and from 78° to 84° in the bottom panel.

daytime and soft precipitation at night is not very clear in the flux and energy plots of Fig. 5, the difference is evident when the energy spectra are compared, as in Fig. 6. In Fig. 6, plots 1 and 2 show the differential energy spectra of typical cusp precipitation. It is characterized by a very high ($>10^7$ (el/cm^2·s·sr·eV)) number flux with the low electron energy range (<100 eV).

On the other hand, the spectrum of soft electron precipitation in the nightside, which may be related to faint auroral arcs in spectrum 3, shows peak flux values ($>10^6$ (el/cm^2·s·sr·eV)) at about 300 eV, dropping sharply above 1 keV. The spectrum 4 may correspond to the discrete arc in the nightside. The energy spectrum 5 in this figure is obtained from the precipitation around 10 MLT as seen in Fig. 5.

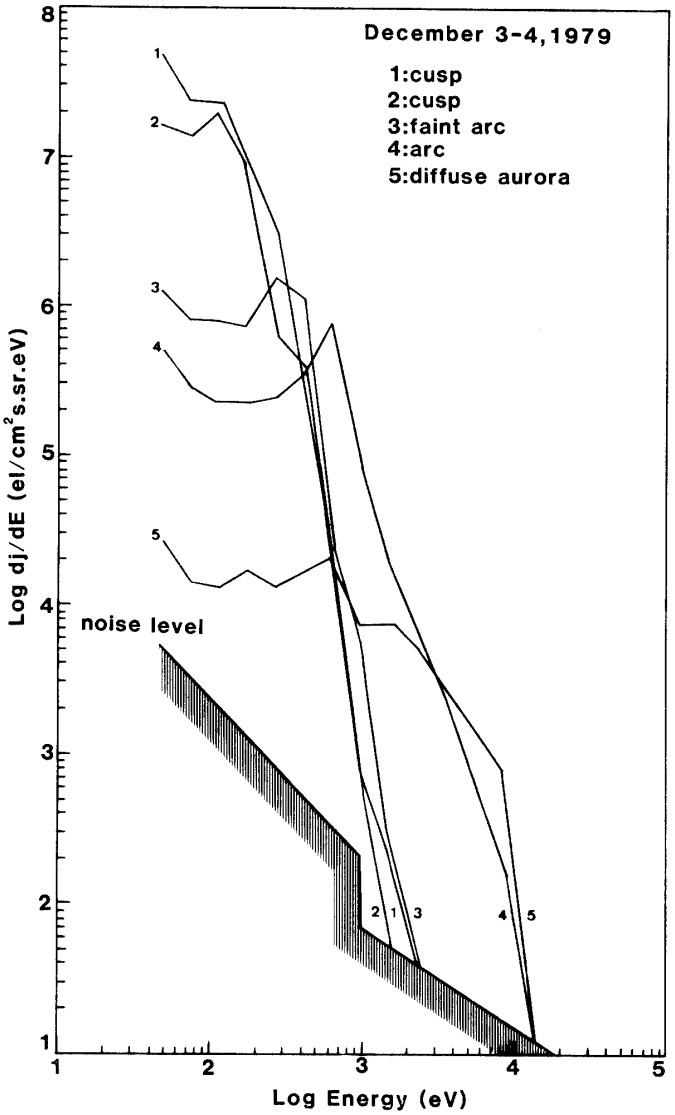

Fig. 6. Electron differential spectra corresponding to cusp (1, 2), faint arc (3), arc (4) and diffuse aurora regions (5). It is noticed that cusp electron differential spectra have intense electron number fluxes in the low energy range (<200 eV). The differential spectra of the faint arc and the discrete arc have a peak flux at energy of a few hundred eV and one keV, respectively.

The characteristics of this spectrum are almost the same as those of spectra 4 in Figs. 2 and 4, which are obtained at lower latitudes in the dawn sector. This suggests that the energy spectrum does not change much as the electrons drift eastward from the dawn sector to the noon sector.

4. Electron Precipitation over the High Latitude Region

Since the boundary between the polar cap and the auroral oval cannot be defined clearly, especially during quiet periods, we use the term "high latitude" to refer to the polar cap and the higher latitude part of the auroral oval in this section.

There are three different kinds of electron precipitation in this region. One of them is polar rain which is usually characterized by a low electron number flux ($<10^6$ (el/cm^2·s·sr·eV)). This phenomenon is reported in a separate paper in this volume. The second is the precipitation related to sun-aligned arcs, whose energy spectrum shows a peak flux at about 300 eV. The third is the precipitation with energy spectra similar to that observed above bright discrete arcs. In this chapter, we show typical examples of electron precipitation observed in the high latitude region in conjunction with sun-aligned arcs and θ auroras.

4.1. Sun-aligned arc electron precipitation

Typical three examples of sun-aligned arcs are shown in Fig. 7. Here, the top panel is a photograph of sun-aligned arcs during a quiet period ($AE \sim 50$ nT), the middle panel is an example during a slightly active period ($AE \sim 300$ nT) and the bottom corresponds to the period of high activity ($AE \gtrsim 400$ nT). Several faint auroral arcs are seen in the top panel. These sun-aligned arcs appeared during a quiet period. The hourly average value of AE index was about 50 nT for this time.

As the magnetic activity increases, the sun-aligned arcs near the center of the polar region disappear while those in the equatorward side remain as shown in the middle panel. During the high magnetic activity period, no clear sun-aligned arc can be seen near the center of the polar region (botom panel). In this interval, the discrete bright arcs can be seen in the dawn and the dusk low latitude regions as seen in the same panel.

In order to examine the characteristics of electron precipitation in the sun-aligned arcs, the electron number flux, energy flux and average energy data are shown in Fig. 8. The top panel shows typical sun-aligned arc precipitation measured by the DMSP-F2 satellite during the interval from 0829 to 0849 in a quiet period. Unfortunately, the precipitation data for the time interval shown in the top panel in Fig. 7 were not available, and the example here is obtained about 20 min later. But the magnetic activity remained low, so that the general distribution of sun-aligned arcs also remained except for some minor changes in individual arcs. The precipitation related to sun-aligned arcs, highly structured, can be seen from 72° to 87° in the night side and from 75° to 86° in the morning side. The bottom panel shows precipitation data obtained in the southern hemisphere during the interval from 1010 to 1030 UT during the orbit after that shown in the top panel. This shows the precipitation for the same time interval exactly the same as shown in the middle panel of Fig. 7. As the magnetic activity increases in this period, the poleward boundary of sun-aligned arc precipitation is found to shift equatorward from 87° (top panel of Fig. 8) to 76° (bottom panel of Fig. 8) in the night side and from 86° to 83° in the morning side. The precipitation patterns in this figure, as well as the auroral pictures in Fig. 7, also include the discrete auroral region and the diffuse auroral region as in the previous examples.

The differential energy spectra corresponding to discrete arcs and a diffuse aurora are shown in Fig. 9. It is evident that the energy spectra for sun-aligned arcs are definitely different from those for discrete and diffuse auroras. The spectra for the sun-aligned arcs have a peak flux at energy of about 300 eV. The discrete arc energy spectrum shown here is almost the same as those in Fig. 4, and that for the diffuse

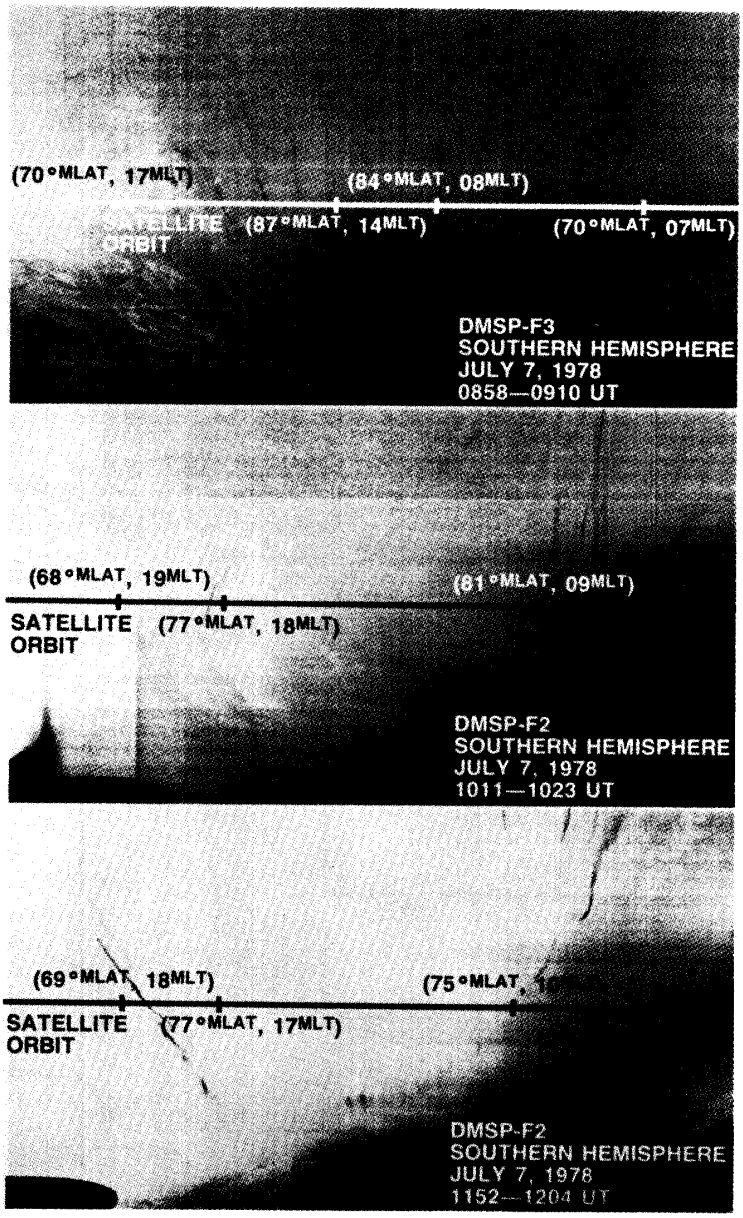

Fig. 7. Auroral image obtained by the DMSP-F2 and F3 satellites. In the top panel, typical sun-aligned arcs can be recognized during a quiet period. As the magnetic activities increased, the sun-aligned arcs gradually disappeared as shown in the middle and bottom panels.

aurora is also similar to the previous diffuse aurora spectrum having no peak in the flux in this energy range. The characteristics of the sun-aligned arc precipitations are similar to those of faint arcs along the poleward part of the auroral oval in the dawn and the dusk sectors in Figs. 2 and 6. The electron precipitation into sun-aligned arcs and that into faint arcs observed on the poleward side of bright discrete arcs are likely to originate from the same electron source.

4.2. θ aurora electron precipitation

A transpolar bright auroral arc can sometimes be seen in the center of the polar cap. This is called θ aurora. (FRANK *et al.*, 1982). Typical examples of θ auroras

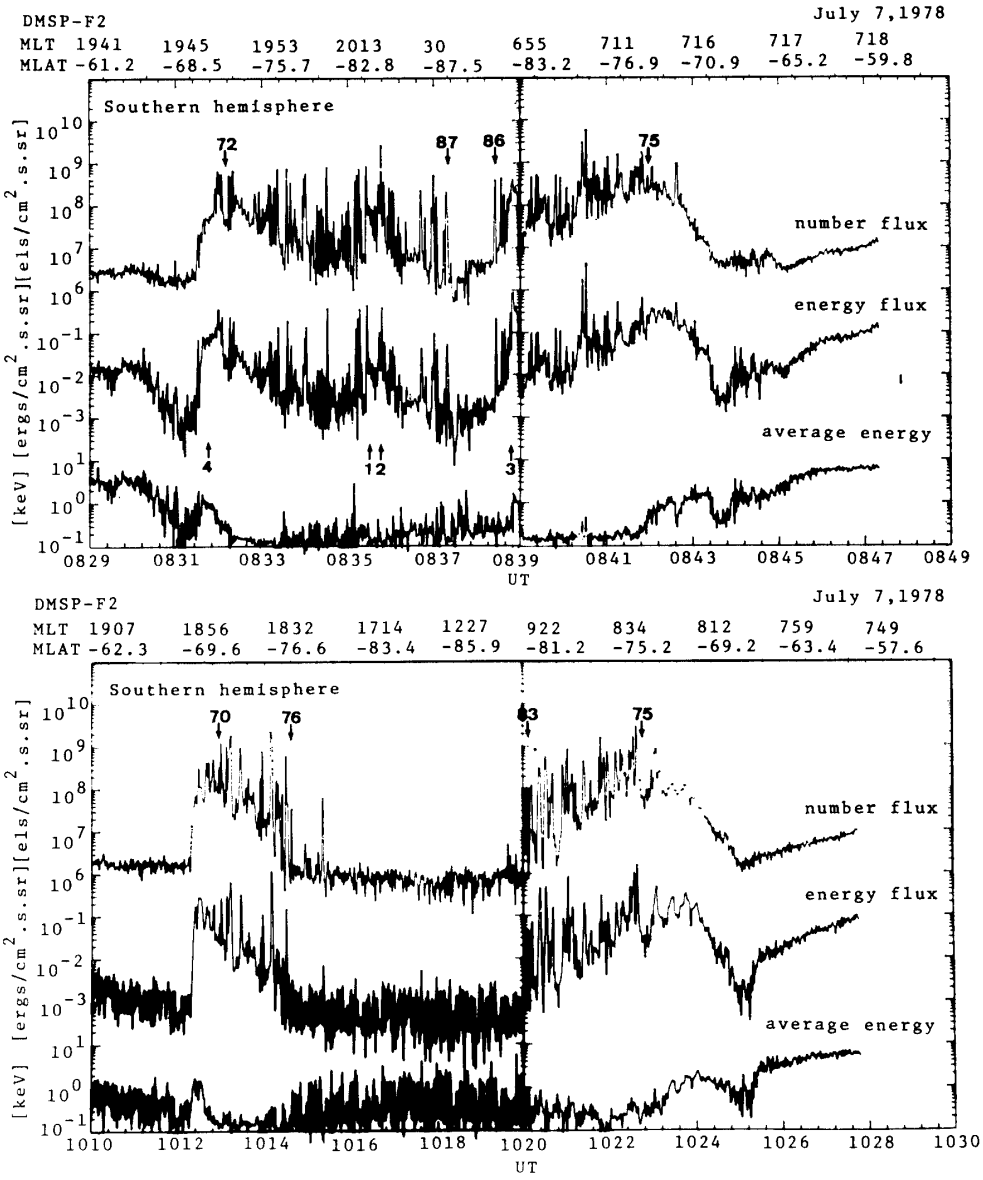

Fig. 8. Electron precipitation data obtained by the DMSP-F2 satellite. In the top panel, a region of sun-aligned arc precipitation can be seen from 72° to 87° on the night side and from 75° to 86° on the morning side. The poleward boundary of the sun-aligned arc precipitation region moves equatorward as the geomagnetic activity increases in the bottom panel.

are shown in Fig. 10, obtained by DMSP-F2 and -F3 satellites in the southern hemisphere. All three examples are obtained during the recovery phase of activity.

In the top panel of the DMSP-F2 auroral image, a bright transpolar discrete aurora can be seen across the center of the polar cap ($\sim 88°$ MLAT) and slightly weak discrete auroras are seen along the dawn and the dusk auroral ovals.

Similar θ auroras are also seen in the middle and the bottom panels. The time interval from the top panel to the bottom panel is nearly two hours. Therefore, the θ auroras very likely lasted for at least 2 hours in this event. It is evident in these figures that the luminosity of the center of the θ aurora was brighter than that of the

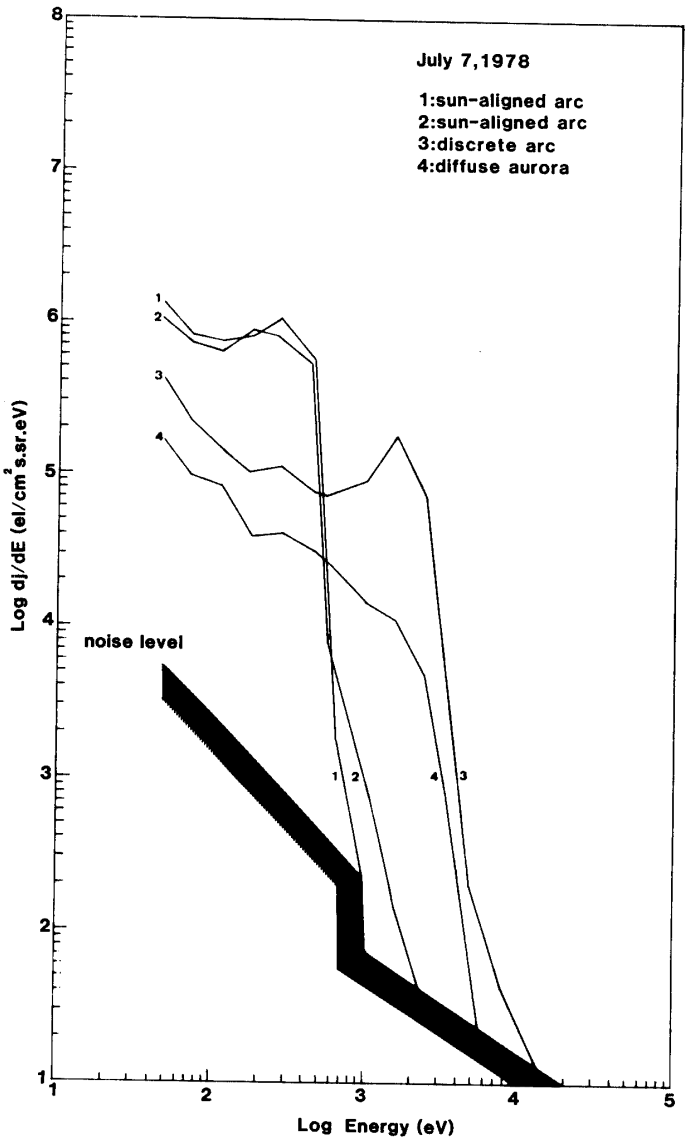

Fig. 9. The differential electron spectra of sun-aligned arcs (1, 2), a discrete arc (3) and a diffuse aurora (4). The spectra of the sun-aligned arcs have a peak flux at an energy of about 300 eV.

oval aurora. It is also found that the location of the central part of the θ aurora moves slightly from the dusk to the dawn sector in this time interval.

The electron precipitation data in this interval are shown in Fig. 11. The three panels show the electron number flux, energy flux and average energy observed along three sequential orbits of DMSP-F2 satellite in the southern and northern hemispheres.

Here again, the time intervals for the middle panels of Figs. 10 and 11 are not exactly the same, and in addition, the middle panel of Fig. 11 is obtained over the northern polar region while that in Fig. 10 is for the southern polar region. However, the stability of the whole auroral system for the time allows us to compare the auroral pattern and the precipitations.

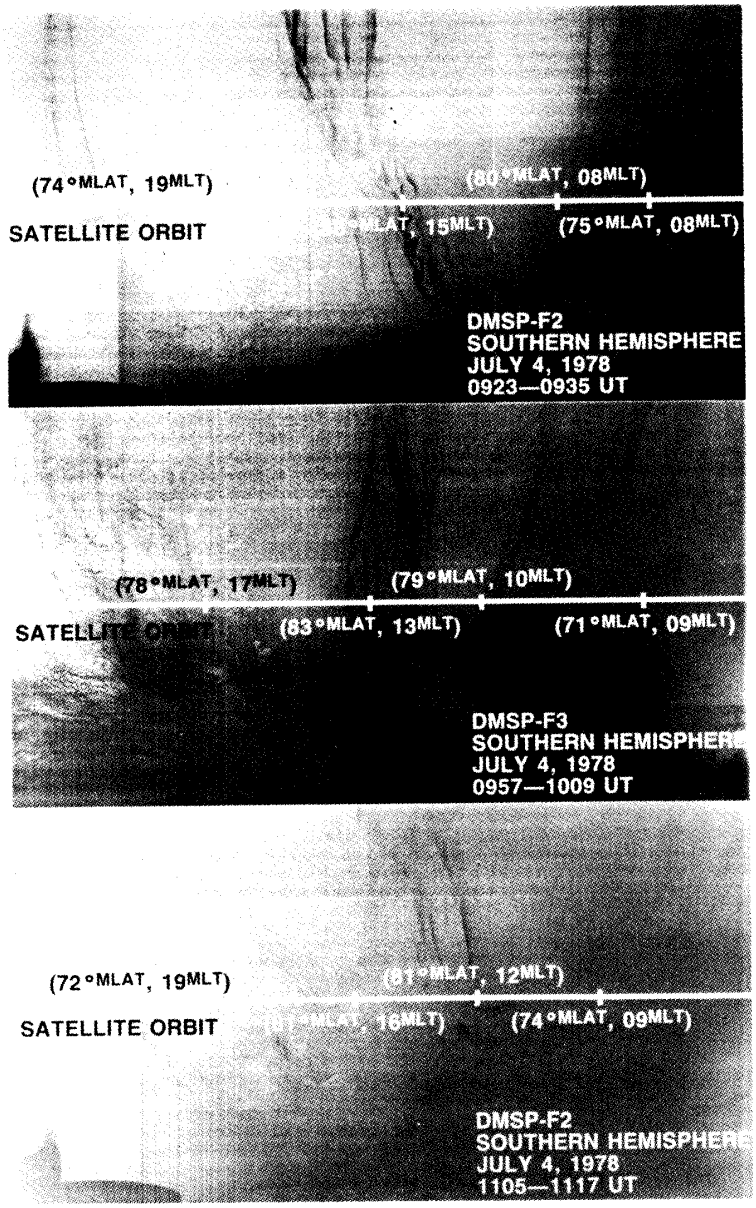

Fig. 10. Sequence auroral images obtained by the DMSP-F2 and F3 satellites. The transpolar aurora seems to be brighter than the discrete auroral arc in the auroral oval.

The top panel shows the electron precipitation data in the southern hemisphere during the interval from 0921 to 0941, obtained simultaneously to the time of the top panel of Fig. 8. Typical electron precipitation at the central part of the θ aurora is seen from 84° in the evening sector to 83° in the morning sector near the center of the polar region. The electron precipitation along the auroral oval is also seen in this panel seen in the evening and morning sectors. The middle panel shows the precipitation data obtained in the northern hemisphere during the interval from 1013 to 1033 UT whereas the corresponding picture of aurora in Fig. 10 (middle panel) was obtained over the southern polar region as mentioned before.

The precipitation pattern in this example is highly structured. Also the separation of the inner part of the θ aurora from the oval is not clear, especially in the

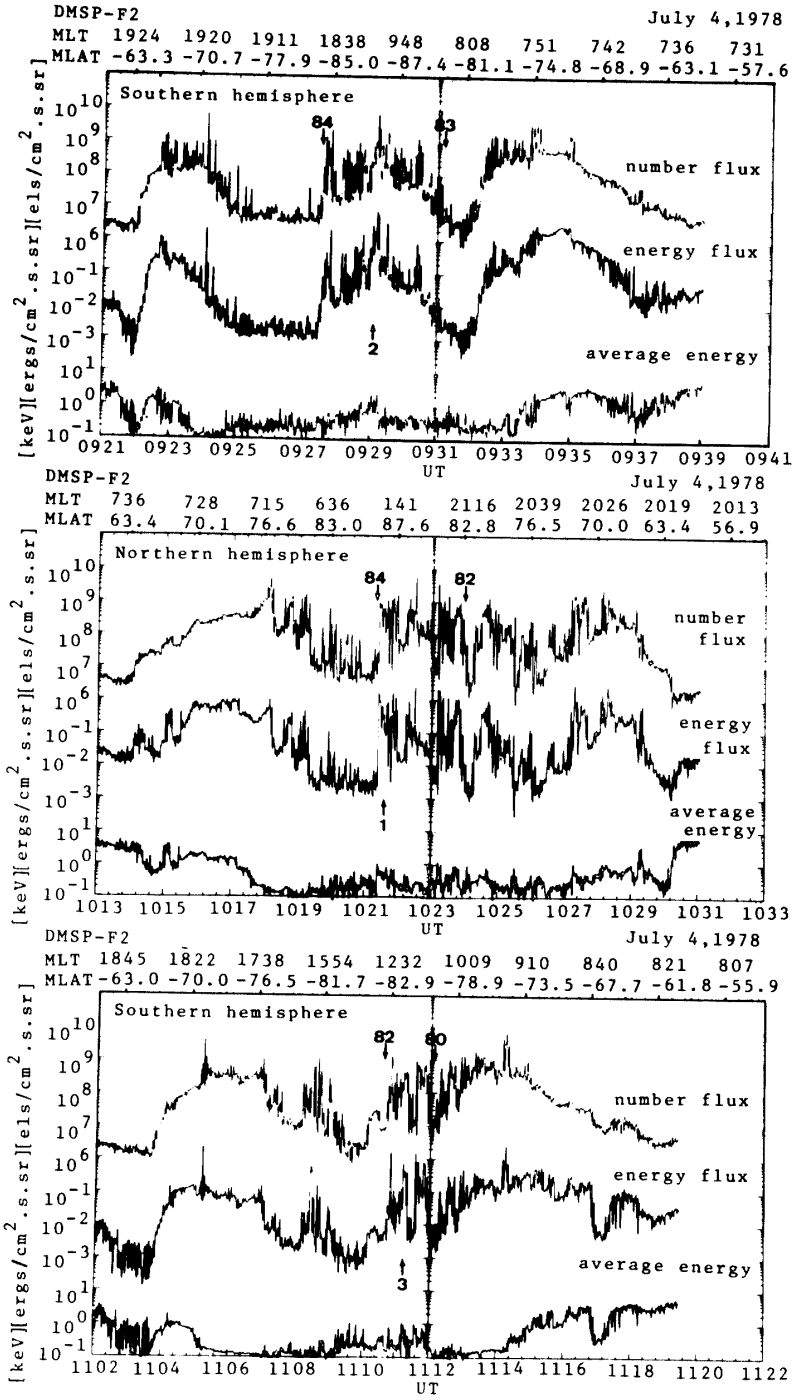

Fig. 11. Electron precipitation data observed by the DMSP-F2 satellite. In the top panel, typical aurora precipitation can be seen from 84° to 83°. In the middle and bottom panels, aurora precipitation can be seen from 84° to 82° and from 82° to 80°, respectively.

dusk sector. Although the high latitude region from 84° in the morning sector to 82° in the evening sector appears to correspond to the inner part of the middle panel of Fig. 10, an exact comparison needs the data in the same hemisphere. What we can say here is that θ aurora electron precipitation as a whole can be simultaneously

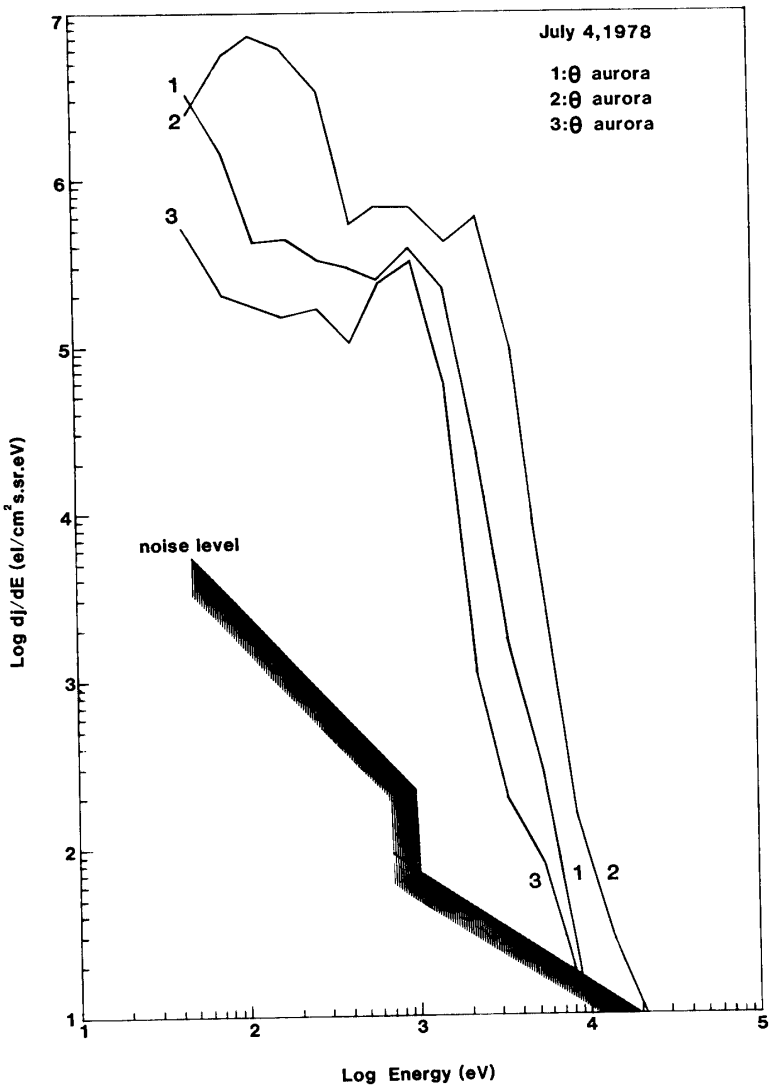

Fig. 12. Differential electron spectra of θ aurora obtained by the DMSP-F2 satellite. The peak number flux of these spectra can be seen at a few keV.

observed in both hemispheres in roughly conjugate areas.

In the bottom panel, the electron precipitation obtained in the southern hemisphere during the interval from 1102 to 1122 UT is shown. The precipitation area from 82° in the evening sector to 80° in the morning sector could correspond to the central part of the θ aurora in the bottom panel of Fig. 10.

The differential energy spectra of the precipitation are shown in Fig. 12. Spectrum 2 was obtained from data shown in the top panel of Fig. 11, spectrum 1 is based on data from the middle panel and spectrum 3 was obtained from data shown in the bottom panel.

The gross features of these spectra are found to be similar. These are some differences in the detailed structure. Note that the energy of the small peak in the number flux decreases from 3 keV to 800 eV from the first to the last orbits, corresponding to the decreases in AE index from 200 to 80 nT for the time. The characteristics of the energy

spectra for the central part of the θ aurora are similar to those of bright discrete aurora in the night and evening side auroral ovals which were shown in Fig. 4.

5. Summary and Conclusion

The characteristics of energy spectra of precipitating electrons over the polar region during quiet and disturbed periods for various local time sectors were examined in this paper. Five different kinds of electron precipitations over the polar region were found in this study. These are summarized as follows:

1) The electron precipitation associated with bright discrete arcs and the transpolar branch of θ auroras.

This electron precipitation shows a clear peak in the electron number flux at an energy between 1 and 7 keV. The auroral luminosity is likely to increase as the peak electron energy increases. The energy spectrum for the transpolar branch of a θ aurora over the polar cap is basically the same as that of the bright discrete arc along the auroral oval. The polar squall precipitation named by WINNINGHAM and HEIKKILA (1974) may be the same as the precipitation here related to the transpolar branch of a θ aurora.

2) The electron precipitation related to the diffuse (possibly pulsating) aurora.

The energy spectra of this kind of precipitation have no clear peaks in number flux in the energy range from 50 eV to 20 keV. They have a higher energy tail. Occasionally, enhancements of electron number flux can be seen at energies higher than 10 keV.

Generally, the precipitation region corresponding to the diffuse aurora and that to the discrete aurora tend to be clearly separated in the morning sector, while these two precipitation regions are frequently mixed in the evening sector.

3) The electron precipitation related to faint arcs in the higher latitude part of the oval and to sun-aligned arcs.

This precipitation has energy spectra with a clear peak in electron number flux at a few hundred eV. The electron number flux near the peak energy range is about 10^6 (el/cm^2·s·sr·eV). The polar shower precipitation reported by WINNINGHAM and HEIKKILA (1974) may be identical with this kind of precipitation.

4) The cusp precipitation

The cusp precipitation is characterized by a large electron number flux ($>10^7$) and by low electron energies (less than 100 eV). The cusp precipitation is observed mostly near the dayside, but sometimes observed in the evening and morning sectors. The cusp-like precipitation in the evening and in the morning has a peak in the electron number flux at energies less than a few hundred eV. A detailed examination of this will be given in a separate paper.

5) The energy spectra of the polar rain

Since the electron number flux of polar rain ($<10^6$ (el/cm^2·s·sr·eV)) is extremely low and is near the threshold level of the DMSP electron detector, it is difficult to examine any polar rain spectra. However, according to WINNINGHAM and HEIKKILA (1974), the spectral structure of the polar rain electrons is identical in shape with that of cusp electrons but is lower in intensity by about 2 orders of magnitude. This homo-

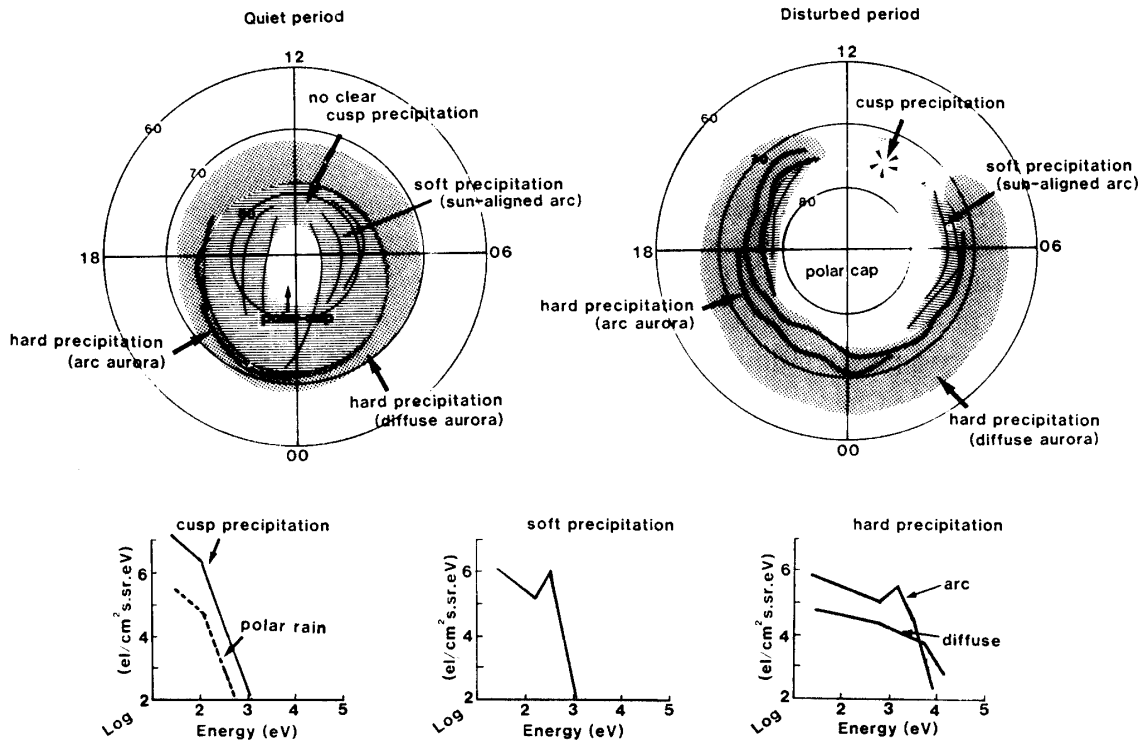

Fig. 13. The top two figures show schematic precipitating electron patterns over the polar region during quiet and the disturbed periods. Cusp, polar rain, soft, and hard differential electron spectra are shown at the bottom.

geneous weak precipitation of electrons is observed clearly over the polar cap region, especially during the disturbed period.

The characteristics of these five different kinds of electron precipitation are summarized in Fig. 13. Generally, different electron precipitation patterns are seen over the polar region during quiet and the disturbed periods. During quiet periods, the hard electron precipitation related to bright discrete arcs and diffuse auroras can be seen near the equatorward part of the auroral oval. The low energy electrons precipitate in relation to the faint arc and the sun-aligned arc in a wide latitudinal range in the poleward part of the auroral oval.

On the other hand, during disturbed periods, the hard precipitation region including discrete and diffuse auroral precipitations, expands both poleward and equatorward, while the region of soft precipitation becomes much narrower. The soft precipitation region sometimes is missing entirely in the night sector. At the same time, the polar rain precipitation region (polar cap region) expands and the typical cusp precipitation can be seen near the dayside.

The energy spectra of these precipitation are schematically illustrated in the bottom panel of Fig. 13. The left spectra show cusp and polar rain precipitation observed in the dayside and in the polar cap, respectively. The middle spectrum shows soft precipitation related to the faint oval arc and the sun-aligned arc obtained in high latitudes during the quiet period. The right two spectra show hard precipitations related to the bright discrete arcs and diffuse auroras.

The difference in the energy spectra of these precipitations must reflect the difference in their sources. The precipitation into the bright discrete arc and the transpolar branch of a θ aurora in the polar cap may originate in the plasma sheet, and possibly may be accelerated by a field-aligned electric field. Our conclusions are consistent with the ion precipitation observations examined by PETERSON and SHELLEY (1984), who claimed that no difference exists between the transpolar branch and the oval. As the average energy of precipitating electrons for the bright discrete arc and the transpolar branch is larger than 1 keV and the peak number flux can be seen around a few keV, these electron precipitations may be identical with the boundary plasma sheet electrons described by WINNINGHAM *et al.* (1975). The precipitation causing the diffuse aurora is likely identical with the central plasma sheet described by WINNINGHAM *et al.* (1975), but it is more likely to be a shell surrounding the earth rather than a sheet in the tail.

On the other hand, the faint discrete arc and/or sun-aligned arc are observed in high latitudes and the average electron energy for these is a few hundred eV. These facts suggest that such kinds of precipitating electrons are related to the magnetospheric boundary layer electrons as reported by HAERENDEL *et al.* (1978).

Cusp electrons here are considered to precipitate directly from the magnetosheath. The average energy of cusp electrons is lower than 100 eV and their number flux in the low energy range ($<$100 eV) is higher than that of the faint discrete arc in the higher latitude part of the oval and above sun-aligned arcs. These results suggest that these low energy electrons come from the magnetospheric entry layer linked to the polar cusp at low altitude. The cusp-like precipitation which is sometimes observed in the evening and morning sectors suggests that the entry layer may sometimes extend or move from the noon sector toward both the dusk and the dawn sectors.

The electron number flux of polar rain is usually very low and homogeneous in its spatial distribution over the entire polar cap. This precipitation may be related to the tail lobe electron in the magnetosphere.

We consider that the five kinds of energy spectra discussed in this paper basically represent the sources of precipitating electrons in the polar region; inner plasma sheet and its boundary layer electrons, magnetospheric boundary layer electron, magnetosheath electron and tail lobe electron. Although the temporal and spatial variations as well as the mutual relationships of precipitation regions and the interplanetary magnetic field were not examined, they must be the key factors in future study in order to understand the solar wind-magnetosphere interactions.

Acknowledgments

The author wishes to thank Dr. C.-I. MENG for his kind and valuable suggestions.

This work was partly supported by Applied Physics Laboratory, The Johns Hopkins University and National Institute of Polar Research in Japan.

References

BURKE, W. J. (1982): Magnetosphere-ionosphere coupling; Contributions from IMS satellite observation. Rev. Geophys. Space Phys., **20**, 685–708.

FRANK, L. A. (1971): Plasma in the Earth's polar magnetosphere. J. Geophys. Res., **76**, 5202–5219.

FRANK, L. A., CRAVEN, J. D., BURCH, J. L. and WINNINGHAM, J. D. (1982): Polar views of the Earth's aurora with Dynamics Explorer. Geophys. Res. Lett., **9**, 1001–1004.

HAERENDEL, G., PASHMAN, G., SCKOPKE, N. and ROSENBAUER, H. (1978): The front side boundary layer of the magnetosphere and the problem of reconnection. J. Geophys. Res., **83**, 3195–3216.

HARDY, D. A., GUSSENHOVEN, M. S. and HUBER, A. (1979): The precipitation electron detectors (SSJ/3) for the block 50/flight 2–5 DMSP satellites; Calibration and data presentation. Rep. AFGL-TR-79-0210, Air Force Geophys. Lab., Hanscom Air Force Base, Bedford.

LASSEN, K. and DANIELSEN, C. (1978): Quiet time pattern of auoral arcs for different directions of the interplanetary magnetic field in the Y–Z plane. J. Geophys. Res., **83**, 5277–5284.

LUI, A. T. Y., VENKATSAN, D., ANGER, C. D., AKASOFU, S.-I., HEIKKILA, W. J., WINNINGHAM, J. D. and BURROWS, J. R. (1977): Simultaneous observations of particle precipitations and auroral emissions by the ISIS 2 satellite in the 19–24 MLT sector. J. Geophys. Res., **82**, 2210–2226.

MAKITA, K., MENG, C.-I. and AKASOFU, S.-I. (1983): The shift of the auroral electron precipitation boundaries in the dawn-dusk sector in association with geomagnetic activity and interplanetary magnetic field. J. Geophys. Res., **88**, 7967–7981.

PETERSON, W. K. and SHELLEY, E. G. (1984): Origin of the plasma in a cross-polar cap auroral feature (theta aurora). J. Geophys. Res., **89**, 6729–6736.

REIFF, P. H. (1983): Polar and aurora phenomena; A review of U. S. progress during 1979–1982. Rev. Geophys. Space. Phys., **21**, 418–433.

SHARP, R. D. and JOHNSON, R. G. (1968): Some average properties of auroral electron precipitation as determined from satellite observations. J. Geophys. Res., **73**, 969–990.

WINNINGHAM, J. D. and HEIKKILA, W. J. (1974): Polar cap auroral electron fluxes observed with ISIS 1. J. Geophys. Res., **79**, 949–957.

WINNINGHAM, J. D., YASUHARA, F., AKASOFU, S.-I. and HEIKKILA, W. J. (1975): The latitudinal morphology of 10 eV to 10 keV electron fluxes during magnetically quiet and disturbed times in the 2100–0300 MLT sector. J. Geophys. Res., **80**, 3148–3171.

(Received October 1, 1984; Revised manuscript received December 12, 1984)